RSC Advances

PAPER

View Article Online
View Journal | View Issue

Cite this: *RSC Adv.*, 2015, **5**, 11223

Synthesis of ordered porous SiO_2 with pores on the border between the micropore and mesopore regions using rosin-based quaternary ammonium salt

Peng Wang,†*[a] Shang-xing Chen,†[a] Zhen-dong Zhao,[b] Zongde Wang[a] and Guorong Fan[a]

A novel, sustainable, rosin-based quaternary ammonium salt, dehydroabietyltrimethyl ammonium bromine, has been applied for the synthesis of ordered hexagonal supermicroporous silica with nanosheet morphology. Unlike the conventional short chain surfactants, rosin-based surfactant possesses a rigid group of a three-ring phenanthrene skeleton. Such a hydrophobic group gives the surfactant a large total volume and small effective headgroup area, which are beneficial for the formation of 2D hexagonal phase. XRD, N_2 adsorption–desorption, TEM, and SEM are used to characterize the samples. The results indicate that the molar ratios of mixture of silicate source, template agent and inorganic acid in the synthesis system have great effects on the regularity of the pore structure. The synthesized material possesses large surface area (1229 m^2 g^{-1}), high pore volume (0.59 cm^3 g^{-1}) and narrow pore size distribution (centered at about 2.03 nm), which is on the borderline between the micropore and mesopore regions. Such a material will be attractive for applications in separations and catalysis because of its potential shape and size selectivities.

Received 10th October 2014
Accepted 19th December 2014

DOI: 10.1039/c4ra12113a

www.rsc.org/advances

1. Introduction

After the scientists of Mobil initially reported the synthesis route of molecular sieves (M41S) in 1992,[1,2] mesoporous materials have been receiving considerable attention because of their potential applications in catalysis, adsorption, biomolecular immobilization, electronic and optoelectronic technologies.[3–6] Such a synthesis route relies on a supermolecular templating mechanism, in which an assembly of amphiphilic surfactants functions as a structure-directing template. A variety of mesoporous materials, such as SBA,[7–9] HMS,[10] MSU[11] and FDU,[12,13] were synthesized using different types of templating agents. Such materials remarkably extended the range of pore sizes attainable for periodic porous materials from 1.2 nm to 2.7–12 nm. Scientists are constantly trying to increase the pore sizes of ordered mesoporous materials for further expansion of their application fields.[14,15] However, few efforts are being devoted to the synthesis of mesoporous materials with small pores. Actually, these materials, which have pores on the border between micropore (D_p < 1.2 nm) and mesopore (D_p > 2.7 nm) regions, are commonly called supermicroporous materials, and they are of great importance because of their shape and size selectivities in most commonly catalyzed reactions such as heavy fraction crude oil processing, new specialty chemical development and new pharmaceutical precursor syntheses.[16,17] As for the current mesoporous materials, their pore sizes (>2.7 nm) are very large to achieve this goal.[6] In addition, the ordered supermicroporous materials also have great potential utilities in the separation and drug delivery fields.[18]

Because the pore sizes of mesoporous materials (M41S) depend on the hydrophobic chain lengths of surfactants, short chain surfactants were applied as the templates to synthesize supermicroporous materials.[19–21] However, the supermicroporous materials prepared with such methods possessed disordered worm-like structures. In order to fix this problem, the mixing templating system was adopted. A surfactant/cosurfactant system of decyltrimethylammonium bromide/butanol was used by Lin *et al.*[22] to successfully synthesize well-ordered super-microporous aluminosilicate. Wang[23] and Zhu *et al.*[24] reported the synthesis of highly ordered supermicroporous silicas with a mixture of short chain cationic–anionic surfactants. Few types of amphiphilic compounds with unique structures were also synthesized and used as templates for the fabrication of supermicroporous materials. Bagshaw

[a]*College of Forestry, Jiangxi Agricultural University, Nanchang, 330045, PR China. E-mail: pengwang1981@126.com*

[b]*Institute of Chemical Industry of Forestry Products, CAF, National Engineering Lab. for Biomass Chemical Utilization, Key and Open Lab. on Forest Chemical Engineering, SFA, Key Lab. of Biomass Energy and Material, Nanjing, Jiangsu Province, 210042, PR China*

† These authors contributed equally to this work and should be considered as co-first authors.

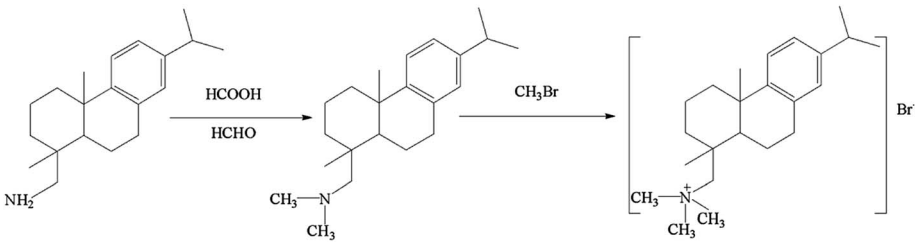

Scheme 1 Synthesis route of dehydroabietyltriethyl ammonium bromine.

et al.[16,25,26] described the synthesis of supermicroporous silica using ω-hydroxyalkylammonium bolaform surfactants. In contrast with the traditional alkylammonium surfactants, the introduction of ω-hydroxyl reduced the micellar radius, which was beneficial for the formation of supermicroporous materials. Ryoo[27] and Wang[28] successively reported the synthesis of supermicroporous materials using short chain gemini surfactants. The abilities of self-assembly of short chain gemini surfactants were stronger than that of corresponding monovalent surfactants; therefore, the highly ordered supermicroporous materials were synthesized. Zhou and coworkers[29,30] investigated the preparation of supermicroporous lamellar silicas with a series of room-temperature ionic liquids (1-alkyl-3-methylimidazolium chloride) as templates *via* the nanocasting technique. The results indicated that the room-temperature ionic liquids could be excellent template agents, and the produced lamellar pore widths varied slightly with the chain lengths of the employed ionic liquids. Semifluorinated surfactants were used as templates by Di *et al.*[31] for the synthesis of ordered hexagonal smaller supermicroporous silicas. Semifluorinated surfactants played a key role in the ultralow temperature synthesis of supermicroporous materials because the common templating (CTAB or P123) systems were completely frozen under such a temperature. Fukasawa *et al.*[32] synthesized the supermicroporous silica using tri(quaternary ammonium) surfactant with a benzene core as the template. In contrast with the conventional surfactant of decyltrimethylammonium bromide, this surfactant was more effective for generating small and regularly arranged pores because of its strong tendency to form cylindrical assemblies. The abovementioned results indicate that the template agents are crucial for the synthesis of supermicroporous materials. Therefore, there is an urgent need for exploring new template agents for the synthesis of supermicroporous materials.

Rosin is a type of an abundant and renewable resource, which has a large variety of uses. The synthesis of surfactants using rosin as a raw material is an important way to the high-valued utilization of rosin. To date, the synthesis of highly ordered silicas using rosin-based surfactants as template agents has not been reported. Unlike traditional surfactants, the rosin-based surfactant possesses a big group of a three-ring phenanthrene skeleton, which is rigid and can be a good candidate for the synthesis of ordered silicas. Moreover, the rosin-based surfactant is derived from natural feedstocks. Low toxicity and renewable properties make it an environmentally friendly reagent for achieving sustainable processes. In this study, a novel self-synthesized rosin-based quaternary ammonium salt, dehydroabietyltrimethyl ammonium bromine (short for DTAB, Scheme 1), was applied as a directing agent to produce highly ordered silicas. The structures of the synthesized samples were characterized using X-ray diffraction, N_2 adsorption and desorption, transmission electron microscopy and scanning electron microscopy.

2. Experimental methods

2.1 Chemicals

Sodium silicate (AR) was purchased from Sinopharm Chemical Reagent Co., Ltd. Hydrochloric acid (AR) was obtained from Shanghai Pilot Test Chemical Industry Co., Ltd. Formaldehyde (AR), formic acid (AR) and acetone (AR) were provided by Nanjing Chemical Reagent Co., Ltd. Methyl bromide (CP) was obtained from Changzhou Institute of Chemistry. Dehydroabietylamine (~95 wt%) was purchased from Hangzhou Wanjing New Materials Co., Ltd.

2.2 Synthesis

2.2.1 Surfactant. Dehydroabietyltrimethyl ammonium bromine was synthesized according to Scheme 1. *N*,*N*-Dimethyl dehydroabietylamine starting from dehydroabietylamine was prepared using the formic acid–formaldehyde method. The procedure involved dissolving dehydroabietylamine in ethanol (95 wt%), followed by adding aqueous formic acid (80 wt%) and formaldehyde (36 wt%). The mole ratio of dehydroabietylamine : formic acid : formaldehyde was 1 : 2 : 2. The obtained solution was stirred at room temperature for 1 h, and then heated under reflux at 353 K for 8 h. After the removal of excess formic acid and formaldehyde, aqueous sodium hydroxide solution (30 wt%) was added until the pH was 12, and the oily precipitate was extracted with dichloromethane. Note that the dichloromethane layer was separated, washed with water until pH = 7, and dried over sodium sulphate. Dichloromethane was removed through vacuum distillation, and *N*,*N*-dimethyl dehydroabietylamine was obtained. Then, *N*,*N*-dimethyl dehydroabietylamine was dissolved in acetone, and CH_3Br was added quickly with stirring at room temperature with the mole ratio of *N*,*N*-dimethyl dehydroabietylamine : CH_3Br = 1 : 2. After 4 h, the dehydroabietyltriethyl ammonium bromine precipitate was obtained and purified by recrystallization three times from a mixture of ethanol and ethyl acetate to give a white solid powder.

2.2.2 Materials. In a typical preparation, a certain amount of sodium silicate and DTAB was dissolved in de-ionized water at 308 K, giving a clear solution. Hydrochloric acid was then added while stirring. The mole composition of the gel was SiO_2 : DTAB : HCl : H_2O = 1.0 : 0.1–0.25 : 1.4–2.1 : 808.0. After further stirring for 24 h, the precipitated products were transferred into a Teflon-lined autoclave and heated at 373 K for 24 h. The products were washed with water and ethanol several times to remove sodium ions and unbound surfactants. After drying at 323 K, the template agent was removed by calcination at 823 K for 4 h at the rate of 1 K min^{-1}.

2.3 Characterization

The crystalline phases of the samples were recorded using an X-ray diffractometer (D8 Focus, Bucker AXS Inc., Germany) with Cu Kα radiation (λ = 0.154 nm). The operating target voltage was 40 kV and the current was 40 mA. The sample was scanned for 2θ ranging from 0.5° to 10.0° for small-angle XRD characterization. Transmission electron microscopy (TEM) images were obtained with a JEOL JEM-2100 instrument operated at an accelerating voltage of 200 kV. Scanning electron microscopy (SEM) images were characterized with a Hitachi S-3400 instrument operated at 15 kV. Porosity and surface area measurements were performed following the N_2 adsorption on a Micromeritics ASAP2020 instrument made by Micromeritics Instrument Corporation. The surface areas were calculated using the Brunauer–Emmett–Teller (BET) model, and pore distributions were plotted using the Barrett–Joyner–Halenda (BJH), Horvath–Kawazoe (HK) and Density Functional Theory (DFT) methods.

3. Results and discussion

The small-angle XRD patterns of the as-synthesized supermicroporous samples prepared with different SiO_2:DTAB mole ratios are shown in Fig. 1. When the SiO_2 : DTAB ratio is 1.0 : 0.1, the sample presents only one diffraction peak (Fig. 1a), indicating that a short-range ordered pore structure is formed. With increase in DTAB dosage, the regularity of the pore structure is considerably enhanced. As the SiO_2:DTAB ratio is 1.0:0.2, the sample (Fig. 1c) reveals three strong peaks at 2θ = 2.98°, 5.17°, 5.91° (d_{100} = 2.96 nm, d_{110} = 1.71 nm, d_{200} = 1.49 nm), which can be related to the (100), (110), and (200) reflections of a long-range ordered 2D hexagonal lattice symmetry (space group 2D-*P6mm*). The values of the interplanar spacing corresponding to the main XRD peak for this sample is 2.96 nm, which is much smaller than that of the normal MCM-41 silicas,[1,2] demonstrating that a type of hexagonal ordered SiO_2 with smaller pores is obtained. However, with further increase in DTAB dosage, the regularity of the pore structure decays. When the optimal regularity is obtained, the concentration of DTAB in the synthesis system is 0.56 wt%. This concentration is rather lower than that of conventional short chain surfactants,[28] suggesting that the self-assembly ability of DTAB is much higher. Small-angle XRD patterns of the as-synthesized mesoporous samples prepared with different

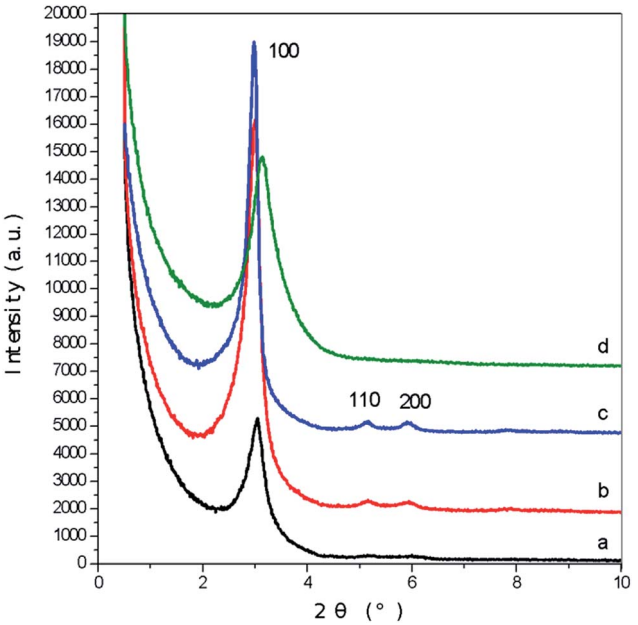

Fig. 1 Small-angle XRD patterns of the as-synthesized supermicroporous silicas prepared with different SiO_2 : DTAB mole ratios, mole ratio: SiO_2 : DTAB : HCl : H_2O = 1.0 : 0.1–0.25 : 1.9 : 808.0, (a): SiO_2 : DTAB = 1.0 : 0.1, (b): SiO_2 : DTAB = 1.0 : 0.15, (c): SiO_2 : DTAB = 1.0 : 0.2, (d): SiO_2 : DTAB = 1.0 : 0.25.

SiO_2 : HCl mole ratios are presented in Fig. 2. With decrease in HCl dosage, the pH of the system increases, and the regularity of the pore structure shows the trend of increase and then decrease, which demonstrates that only a suitable pH

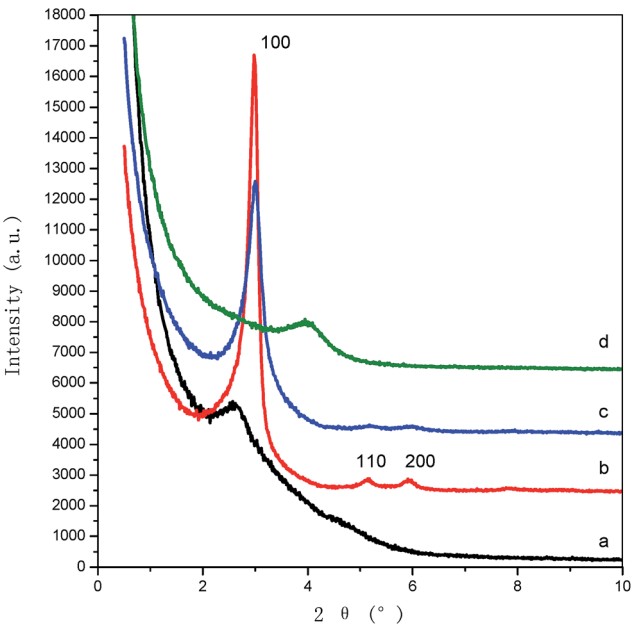

Fig. 2 Small-angle XRD patterns of as-synthesized mesoporous silicas prepared with different SiO_2 : HCl mole ratios, mole ratio: SiO_2 : DTAB : HCl : H_2O = 1.0 : 0.2 : 1.4–2.1 : 808.0, (a): SiO_2 : HCl = 1.0 : 2.1, (b): SiO_2 : HCl = 1.0 : 1.9, (c): SiO_2 : HCl = 1.0 : 1.7, (d): SiO_2 : HCl = 1.0 : 1.4.

value (~8.5) can enhance the regularity of the pore structures. Fig. 3 shows the small-angle XRD patterns of the as-synthesized and calcined samples prepared with mole ratio of SiO_2 : DTAB : HCl : H_2O = 1.0 : 0.2 : 1.9 : 808.0. After calcination at 823 K, three peaks at $2\theta = 3.11°$, 5.33°, 6.14° (d_{100} = 2.84 nm, d_{110} = 1.66 nm, d_{200} = 1.44 nm) can be observed in Fig. 3b, indicating that the hexagonal pore structure is maintained after calcination. Due to the removal of surfactants, the peaks sharpen with stronger intensities. The small-angle peaks of the calcined sample shift to higher angles, which can be related to the shrinkage of unit cell upon calcination. The primary pore sizes (W_d) of materials with a hexagonally ordered array of uniform pores can be evaluated according the equation of $W_d = cd_{100}[\rho V_p/(1 + \rho V_p)]^{1/2}$ using the XRD (100) interplanar spacing, and primary pore volume results, where ρ is 2.2 g cm^{-3} (the pore wall density for amorphous silica), and c is 1.213 (a constant for cylindrical pores).[27] For the calcined sample, the pore size calculated is 1.93 nm, suggesting that the supermicropores are obtained.

Fig. 4 presents the TEM images of the as-synthesized and calcined supermicroporous silicas prepared with the mole ratio of SiO_2 : DTAB : HCl : H_2O = 1.0 : 0.2 : 1.9 : 808.0. Fig. 4a shows the pore structure along the [110] direction. The sample displays well-ordered curved pores with walls perfectly parallel to each other. The curved pores may be caused by the bending of the nanosheeted silicas (Fig. 5). It can be seen that Fig. 4b ([001] direction) displays uniform channels of 2D hexagonal structure and the regular arrays running along a large domain, suggesting that the structure is in a highly ordered arrangement. After calcination, the structure is still maintained (Fig. 4c and d). Note that the pore size of the calcined sample is about 2.0 nm, and the width of pore wall is about 1.0 nm. Particle morphology as determined by the SEM method is shown in Fig. 5. It can be seen that the sample is made of well-dispersed nanosheets without any agglomeration.

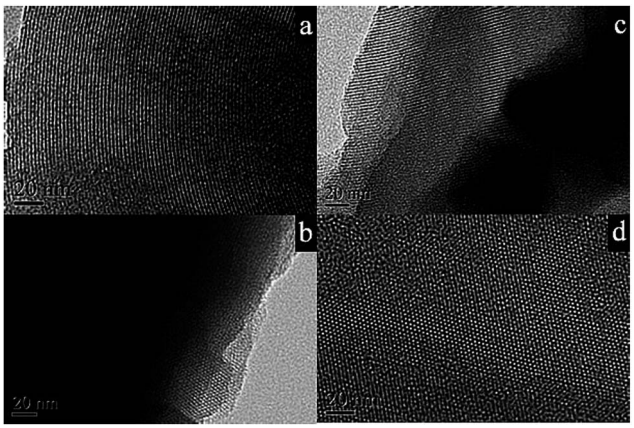

Fig. 4 TEM images of as-synthesized (a and b) and calcined (c and d) supermicroporous silicas prepared with a mole ratio of SiO_2 : DTAB : HCl : H_2O = 1.0 : 0.2 : 1.9 : 808.0 taken in [110] (a and c) and [001] (b and d) directions.

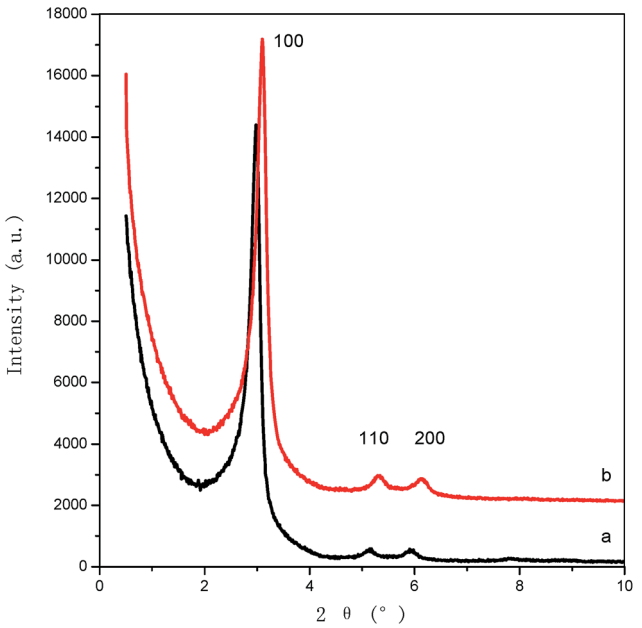

Fig. 3 Small-angle XRD patterns of the as-synthesized (a) and calcined (b) supermicroporous silicas prepared with a mole ratio of SiO_2 : DTAB : HCl : H_2O = 1.0 : 0.2 : 1.9 : 808.0.

Fig. 6a plots the N_2 adsorption–desorption isotherm of the calcined sample synthesized with mole ratio of SiO_2 : DTAB : HCl : H_2O = 1.0 : 0.2 : 1.9 : 808.0. The sample exhibits a transitional type between typical I and IV curves according to the IUPAC classification.[33] A clear capillary condensation step occurs at a relative pressure (P/P_0) of 0.15, which is rather lower than that obtained for any of the previously reported mesoporous materials, suggesting that supermicropores exist in the resulting sample. In Fig. 6a, a linear range for P/P_0 can be observed between 0.04 and 0.15. When P/P_0 is higher than 0.15, a deviation from linearity can be found. Thus, the P/P_0 range of 0.04–0.15 should be selected to calculate the BET surface area. The BET surface area of the sample is 1229 m^2 g^{-1}, and the pore volume is 0.59 cm^3 g^{-1}. Since the precise determination of the pore size distributions

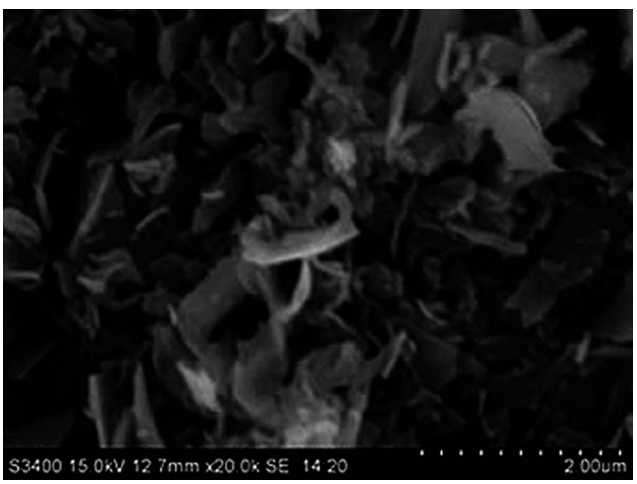

Fig. 5 SEM image of calcined supermicroporous silica prepared with a mole ratio of SiO_2 : DTAB : HCl : H_2O = 1.0 : 0.2 : 1.9 : 808.0.

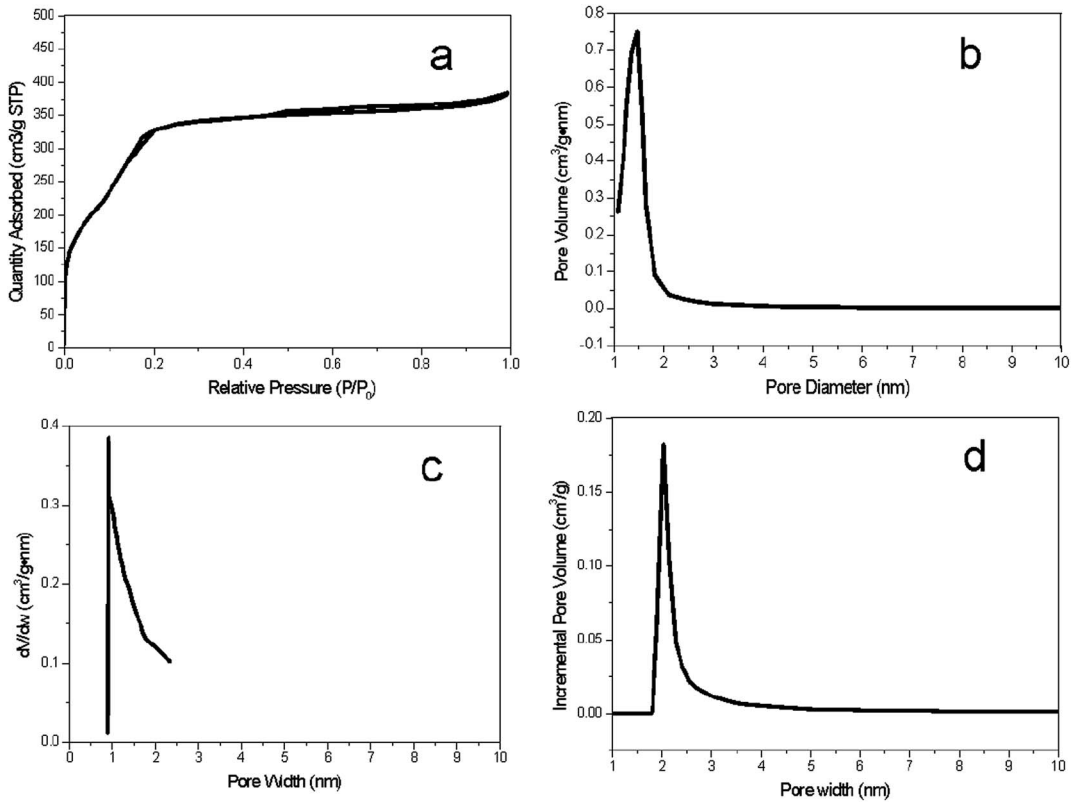

Fig. 6 N_2 adsorption–desorption isotherm (a) and pore size distributions (BJH: (b), HK: (c), DFT: (d)) of calcined supermicroporous silica prepared with a mole ratio of SiO_2 : DTAB : HCl : H_2O = 1.0 : 0.2 : 1.9 : 808.0.

for material in supermicroporous regions is still a matter of uncertainty,[27] the pore size distributions of the sample are calculated from the adsorption branch of isotherm using the BJH (Fig. 6b), HK (Fig. 6c) and DFT models (Fig. 6d). The sample shows a narrow pore diameter distribution centered at about 1.47 nm for the BJH model, 1.13 nm for the HK model and 2.03 nm for the DFT model. Regardless of the models that are employed, the pore sizes obtained are obvious in the supermicroporous regions. However, according to the results evaluated by XRD (100) interplanar spacing and the TEM characterization, the result calculated by DFT model are more reliable. According to the formula $a_0 = 2d/3^{0.5}$ ($d_{100} = 2.84$ nm), the size of the hexagonal unit cell is 3.28 nm, and the width of pore wall is 1.25 nm, which agrees with the TEM results. It is almost impossible to synthesize well-ordered supermicroporous materials using traditional short chain surfactants without any additive agents because their hydrophobic chains are too short to properly maintain good micellar structures in an aqueous environment,[19–21] and their large effective headgroup areas prevent their formation of 2D hexagonal phases.[9,27] Unlike the conventional short chain surfactants, rosin-based surfactant possesses a rigid group of a three-ring phenanthrene skeleton, which gives the surfactant a large total volume. Moreover, such a hydrophobic group has a strong steric effect by which the effective headgroup area of the surfactant is suppressed; therefore, the 2D hexagonal phase is easily formed.

4. Conclusions

Ordered hexagonal supermicroporous silica with nanosheet morphology has been successfully synthesized with a type of novel sustainable rosin-based quaternary ammonium salt, dehydroabietyltrimethyl ammonium bromine. Unlike the conventional short chain surfactants, the rosin-based surfactant possesses a rigid group of a three-ring phenanthrene skeleton. Such a hydrophobic group gives the surfactant a large total volume and small effective headgroup area, which are beneficial for the formation of the 2D hexagonal phase. The regularity of the pore structure is found to strongly depend on the mole ratio of the mixture of silicate source, template agent and inorganic acid. The synthesized material possesses large surface area, high pore volume and narrow pore size distribution, which is on the borderline between the micropore and mesopore regions. Such a material will be attractive for applications in separations and catalysis because of its potential shape and size selectivities.

Acknowledgements

This work was supported by the Research Fund for the Doctoral Program of Higher Education of China (grant no. 20133603120002).

References

1 J. Beck, J. Vartuli, W. Roth, M. Leonowicz, C. Kresge, K. Schmitt, C. Chu, D. Olson and E. Sheppard, *J. Am. Chem. Soc.*, 1992, **114**, 10834–10843.
2 C. Kresge, M. Leonowicz, W. Roth, J. Vartuli and J. Beck, *Nature*, 1992, **359**, 710–712.
3 E. J. Crossland, N. Noel, V. Sivaram, T. Leijtens, J. A. Alexander-Webber and H. J. Snaith, *Nature*, 2013, **495**, 215–219.
4 J. Fan, C. Yu, F. Gao, J. Lei, B. Tian, L. Wang, Q. Luo, B. Tu, W. Zhou and D. Zhao, *Angew. Chem.*, 2003, **115**, 3254–3258.
5 C. Charnay, S. Bégu, C. Tourné-Péteilh, L. Nicole, D. A. Lerner and J.-M. Devoisselle, *Eur. J. Pharm. Biopharm.*, 2004, **57**, 533–540.
6 A. Corma, *Chem. Rev.*, 1997, **97**, 2373–2420.
7 D. Zhao, J. Feng, Q. Huo, N. Melosh, G. H. Fredrickson, B. F. Chmelka and G. D. Stucky, *Science*, 1998, **279**, 548–552.
8 C. Yu, B. Tian, J. Fan, G. D. Stucky and D. Zhao, *J. Am. Chem. Soc.*, 2002, **124**, 4556–4557.
9 Q. Huo, D. I. Margolese and G. D. Stucky, *Chem. Mater.*, 1996, **8**, 1147–1160.
10 P. T. Tanev and T. J. Pinnavaia, *Science*, 1995, **267**, 865–867.
11 S. A. Bagshaw, E. Prouzet and T. J. Pinnavaia, *Science*, 1995, **269**, 1242–1244.
12 X. Liu, B. Tian, C. Yu, F. Gao, S. Xie, B. Tu, R. Che, L. M. Peng and D. Zhao, *Angew. Chem., Int. Ed.*, 2002, **41**, 3876–3878.
13 C. Yu, Y. Yu and D. Zhao, *Chem. Commun.*, 2000, 575–576.
14 G. Zhou, Y. Chen, J. Yang and S. Yang, *J. Mater. Chem.*, 2007, **17**, 2839–2844.
15 J. Fan, C. Yu, L. Wang, B. Tu, D. Zhao, Y. Sakamoto and O. Terasaki, *J. Am. Chem. Soc.*, 2001, **123**, 12113–12114.
16 S. Bagshaw and A. Hayman, *Adv. Mater.*, 2001, **13**, 1011–1013.
17 M. E. Davis, *Nature*, 2002, **417**, 813–821.
18 P. Horcajada, A. Ramila, J. Perez-Pariente and M. Vallet-Regı, *Microporous Mesoporous Mater.*, 2004, **68**, 105–109.
19 J. Beck, J. Vartuli, G. Kennedy, C. Kresge, W. Roth and S. Schramm, *Chem. Mater.*, 1994, **6**, 1816–1821.
20 M. Kruk, M. Jaroniec and A. Sayari, *J. Phys. Chem. B*, 1997, **101**, 583–589.
21 D. P. Serrano, J. Aguado and E. Garagorri, *Chem. Commun.*, 2000, 2041–2042.
22 Y.-S. Lin, H.-P. Lin and C.-Y. Mou, *Microporous Mesoporous Mater.*, 2004, **76**, 203–208.
23 R.-L. Wang, Y.-M. Zhu, X.-M. Zhang, H.-W. Ji, L. Li and H.-Y. Ge, *J. Colloid Interface Sci.*, 2013, **407**, 128–132.
24 Y.-M. Zhu, R.-L. Wang, W.-P. Zhang, H.-Y. Ge and L. Li, *Chem. Lett.*, 2014, **43**, 1170–1172.
25 S. A. Bagshaw and A. R. Hayman, *Microporous Mesoporous Mater.*, 2001, **44**, 81–88.
26 S. A. Bagshaw and A. R. Hayman, *Chem. Commun.*, 2000, 533–534.
27 R. Ryoo, I. S. Park, S. Jun, C. W. Lee, M. Kruk and M. Jaroniec, *J. Am. Chem. Soc.*, 2001, **123**, 1650–1657.
28 R. Wang, S. Han, W. Hou, L. Sun, J. Zhao and Y. Wang, *J. Phys. Chem. C*, 2007, **111**, 10955–10958.
29 Y. Zhou and M. Antonietti, *Adv. Mater.*, 2003, **15**, 1452–1455.
30 Y. Zhou and M. Antonietti, *Chem. Mater.*, 2004, **16**, 544–550.
31 Y. Di, X. Meng, L. Wang, S. Li and F.-S. Xiao, *Langmuir*, 2006, **22**, 3068–3072.
32 Y. Fukasawa, A. Sugawara, H. Hirahara, A. Shimojima and T. Okubo, *Chem. Lett.*, 2010, **39**, 236–237.
33 S. Brunauer, L. S. Deming, W. E. Deming and E. Teller, *J. Am. Chem. Soc.*, 1940, **62**, 1723–1732.

